Resonant energy transfer in quantum dots: Frequency-domain luminescent spectroscopy

S. Yu. Kruchinin,* A. V. Fedorov,† and A. V. Baranov
Saint-Petersburg State University of Information Technologies, Mechanics and Optics, 49 Kronverksky Avenue, 197101 St. Petersburg, Russia

T. S. Perova
Department of Electronic and Electrical Engineering, Trinity College, University of Dublin, Dublin 2, Ireland

K. Berwick
Department of Electronic and Communications Engineering, Dublin Institute of Technology, Dublin 8, Ireland
(Received 23 April 2008; published 11 September 2008)

The resonant energy transfer due to weak electrostatic interaction in a system of two quantum dots has been theoretically investigated. The probability of this process in the case of a direct-gap semiconductor has been calculated assuming that the interaction between the quantum dot donor electrons and the quantum dot acceptor electrons is described by a screened Coulomb potential. This allows one to consider all the important multipole terms of the interaction and to correctly analyze the dipole-forbidden transitions. It has been found that the energy transfer from the donor to the dipole-forbidden states of the acceptor plays an essential role in the process. The anisotropy and temperature dependence of the energy transfer have been analyzed. Analytical expressions for the luminescent spectra of two interacting quantum dots experiencing resonant energy transfer have been derived.

DOI: 10.1103/PhysRevB.78.125311 PACS number(s): 78.67.Hc, 78.55.−m, 73.21.La

I. INTRODUCTION

The investigation of nonradiative resonant energy transfer between pairs of spatially separated quantum objects, such as atoms, molecules, impurity centers, or nanostructures, is one of the most important problems in solid-state physics.[1–3] In recent years, this phenomenon in quantum dot (QD) systems has been extensively studied both experimentally and theoretically.[4–11] This interest is stimulated by predicted future technological applications such as luminescent markers and sensors,[12,13] low-threshold lasers,[14] cellular automata,[15] and quantum computers.[16–18] In addition, an ensemble of quantum dots is a good model for the detailed investigation of the basic physics of nonradiative energy-transfer phenomena. Because of the quantum size effect,[19] one can generate a resonance condition between arbitrary electronic states of the QD donor and QD acceptor by choosing quantum dots of a suitable size and shape. This allows the investigation of the dependence of energy-transfer efficiency on the properties of the electronic states involved in this process.

An early theoretical description of nonradiative resonant energy transfer in molecular systems was developed by Förster.[20] He assumed that energy transfer occurs primarily due to weak dipole-dipole interaction. This interaction is considered to be sufficiently weak that perturbation of the molecular energy spectrum does not occur. So, the energy-transfer probability can be calculated using first-order perturbation theory for a continuous spectrum[21] (the so-called Fermi's golden rule). Förster theory[20] has been generalized by Dexter[22] to the cases of quadrupole and exchange interactions.

The dipole-dipole approximation has been frequently used for theoretical modeling of the energy transfer in QD systems[8,9,23] and for interpretation of experimental data.[4,10,24,25] Certainly, the dipole-dipole approximation gives an adequate description of the energy transfer if the distance between quantum dots is much larger than their size. But, questions arise as to the validity of this approximation in the commonly occurring case when the quantum dots are separated by distances comparable to their size. In this situation, one should consider higher-order multipole interactions. The simplest way to do this is to assume that the interaction of the electronic subsystems of the donors and acceptors is described by the Coulomb potential, while dielectric screening is allowed for by an effective dielectric constant, independent of position. This approach has been used in recent theoretical works.[11,16] For example, in Ref. 16 a numerical calculation has shown that the dipole-dipole approximation is valid even for short distances between cube shaped quantum dots. However, when an attempt is made to extend this approximation to QDs of cuboid shape, significant errors appear. Energy-transfer rates for spherical quantum dots in direct- and indirect-gap semiconductors have been numerically calculated using a tight-binding method.[11] It has been found that the dipole-dipole approximation is adequate for direct-gap semiconductors even at short interdot distances. In the case of indirect-gap semiconductors, multipolar interactions are more important over short distances, nevertheless the dipole-dipole interaction still dominates.

However, these results conflict with simple estimates of the relative contribution of dipole-quadrupole interactions to energy transfer in a system of contacting spherical quantum dots based on the well-known relation $W_{dq}/W_{dd}=(a/r)^2$, where W_{dq} and W_{dd} are the probabilities of dipole-quadrupole and dipole-dipole energy transfer, respectively, a is the dipole arm, and r is the distance between dipoles.[1,22] It gives $W_{dq}/W_{dd}=1/4$ for quantum dots of radius R.

We analyze this contradiction in this work, where we consider the nonradiative resonant energy transfer between two spherical quantum dots, coupled by a screened Coulomb po-

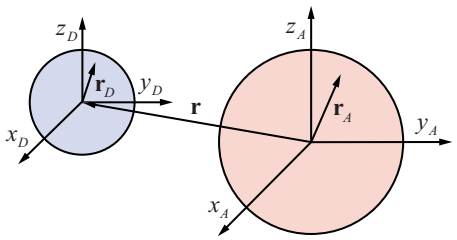

FIG. 1. (Color online) Coordinate systems of two interacting quantum dots.

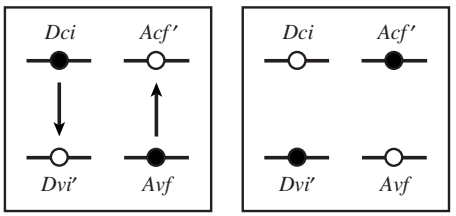

FIG. 2. Electronic configuration of initial and final states of resonant energy-transfer process. Black circles correspond to an occupied electronic state; white circles depict an empty state. Symbols D and A denote the electronic levels of the donors and acceptors in the conduction c and valence v bands; i,i',f,f' are the quantum numbers.

tential interaction. Selection rules for the interband transitions due to energy transfer were obtained and also a relatively simple expression for the matrix element of the interdot interaction. We found that dipole-dipole approximation correctly describes the energy transfer between spherical dots when transitions in both donors and acceptors are dipole allowed. However, when the dipole-forbidden transition is involved in the energy transfer, the relative contribution of the multipole terms to the process can be as high as 25% for contacting quantum dots. A further aim of this work was to analyze distance and temperature dependencies of the luminescence spectra of two interacting quantum dots. In spite of the importance of this problem for interpretation of experimental data, it has, to the best of our knowledge, never been done via this unified approach.

The paper is organized as follows. The calculation of the matrix element of energy transfer induced by Coulomb interaction and an analysis of its dependence on the interdot distance and dipole moment orientation are outlined in Sec. II. We also propose here a generalization of our results to the case of quantum dots with finite potential walls. Section III contains the derivation of the energy-transfer rate together with an analysis of its dependence on temperature. In Sec. IV, we develop the theory of stationary luminescence from two interacting quantum dots and perform an analysis of the dependence of the luminescence spectra on interdot distance. Concluding remarks are given in Sec. V. Appendix contains details of the calculation of the interdot matrix element and a more detailed discussion of the selection rules for the interband transitions due to energy transfer.

II. ENERGY-TRANSFER MATRIX ELEMENT

We consider a spherical quantum dot donor and a quantum dot acceptor with radii R_D and R_A, respectively, separated by a distance $\mathbf{r}$ (see Fig. 1). We assume that the quantum dots are embedded in a dielectric matrix, so we can use an infinite potential wall model. These approaches adequately describe the electronic structure of spherical semiconductor nanocrystals formed in organic and aqueous solutions by the hot-injection method.[4,26] The systems formed from such nanocrystals demonstrate the energy-transfer properties and hold much promise for biosensoring and light harvesting applications.[4,27,28] In the initial state of this system there is an electron in the conduction band of the donor and the acceptor in valence band is fully populated (Fig. 2). As a result of interdot Coulomb interaction described by the potential,

$$V(\mathbf{r},\mathbf{r}_D,\mathbf{r}_A) = \frac{e^2}{\varepsilon|\mathbf{r}+\mathbf{r}_D-\mathbf{r}_A|}, \tag{1}$$

this system passes into a final state with an electron in the valence band of the donor and an electron in the conduction band of the acceptor (Fig. 2). In expression (1) $\mathbf{r}_D$ and $\mathbf{r}_A$ are the radius vectors of electrons, originated at the centers of the corresponding quantum dots, $\mathbf{r}$ is the vector directed from the center of the acceptor to the center of the donor. From Ref. 11, screening of the Coulomb potential is taken into account by the use of an effective dielectric constant, which ε is determined by the high-frequency dielectric constants of the donor ε_D, acceptor ε_A, and matrix ε_M,

$$\varepsilon = \frac{(\varepsilon_D+2\varepsilon_M)(\varepsilon_A+2\varepsilon_M)}{9\varepsilon_M}. \tag{2}$$

The matrix element of the energy transfer (see Fig. 2) due to interdot Coulomb interaction can be expressed as follows:

$$\begin{aligned} M_{DA} &\equiv \langle i',f'|V|i,f\rangle \\ &= \frac{e^2}{\varepsilon}\int\int d^3r_D d^3r_A \\ &\quad \times \frac{\Psi^*_{Dvi'}(\mathbf{r}_D)\Psi^*_{Acf}(\mathbf{r}_A)\Psi_{Dci}(\mathbf{r}_D)\Psi_{Avf'}(\mathbf{r}_A)}{|\mathbf{r}+\mathbf{r}_D-\mathbf{r}_A|}, \end{aligned} \tag{3}$$

where $\Psi_{\alpha\varkappa t}(\mathbf{r}_\alpha)$ is the wave function of donor $\alpha=D$ (acceptor $\alpha=A$) in band $j=c,v$ in a state with quantum numbers $t=i,i'$ (donor) or $t=f,f'$ (acceptor). We neglect the exchange term in Eq. (3) because it is insignificant.[16,29]

In this calculation, we consider a strong confinement mode,[19] neglect the intradot Coulomb interaction, and use a two-band model of semiconductor electronic structure. Using an effective-mass method,[30] the wave function of the carrier $\Psi_{\alpha\varkappa t}(\mathbf{r})=u_{\alpha\varkappa}(\mathbf{r})\psi_{\alpha\varkappa t}(\mathbf{r})$ is given by the product of the Bloch amplitude and the envelope wave function $\psi_{\alpha\varkappa t}$. For spherical quantum dots with infinite potential barriers the envelope is determined by the expression

$$\psi_{\alpha\varkappa t}(\mathbf{r}_\alpha) = \sqrt{\frac{2}{R_\alpha^3}} \frac{j_{l_\alpha}(\xi_{n_\alpha l_\alpha} r_\alpha / R_\alpha)}{j_{l_\alpha+1}(\xi_{n_\alpha l_\alpha})} Y_{l_\alpha m_\alpha}(\vartheta_\alpha, \varphi_\alpha), \tag{4}$$

where $t=\{nlm\}$, n, l, m are the principal quantum number, angular momentum, and its projection, respectively, R is the radius of quantum dot, $j_l(x)$ are the spherical Bessel functions, Y_{lm} are the spherical harmonics, and ξ_{nl} is the nth root of equation $j_l(x)=0$.

To allow the separation of the integration variables, we use the following Fourier expansion:

$$\frac{1}{|\mathbf{r}+\mathbf{r}_D-\mathbf{r}_A|} = \frac{1}{2\pi^2}\int d^3q \frac{e^{i\mathbf{q}(\mathbf{r}+\mathbf{r}_D-\mathbf{r}_A)}}{q^2}.$$

Now, matrix element (3) will be

$$M_{DA} = \frac{e^2}{\varepsilon}\frac{1}{2\pi^2}\int d^3q \frac{e^{i\mathbf{qr}}}{q^2} S^{(D)}_{ii'}(\mathbf{q}) S^{(A)*}_{f'f}(\mathbf{q}),$$

where

$$S^{(\alpha)}_{tt'}(\mathbf{q}) = \int d^3r_\alpha \Psi^*_{\alpha vt'}(\mathbf{r}_\alpha) e^{i\mathbf{qr}_\alpha} \Psi_{\alpha ct}(\mathbf{r}_\alpha). \tag{5}$$

Let us express $\mathbf{r}_\alpha$ as the sum of the radius vector of an elementary cell $\mathbf{r}_{k_\alpha}$ and the radius vector of the electron inside the cell $\mathbf{r}'_\alpha$. We use the following properties of Bloch amplitudes and envelope functions:

$$\psi_{\alpha\varkappa t}(\mathbf{r}_{k_\alpha}+\mathbf{r}'_\alpha) \approx \psi_{\alpha\varkappa t}(\mathbf{r}_{k_\alpha}), \quad u_{\alpha\varkappa}(\mathbf{r}_{k_\alpha}+\mathbf{r}'_\alpha) = u_{\alpha\varkappa}(\mathbf{r}'_\alpha).$$

We can replace the integral over the volume of the quantum dots V_α by a sum of integrals over the volumes of elementary cells Ω_α in Eq. (5),

$$S^{(\alpha)}_{tt'}(\mathbf{q}) = \sigma^{(\alpha)}_{tt'}\frac{1}{\Omega_\alpha}\int d^3r'_\alpha u^*_{\alpha v}(\mathbf{r}'_\alpha) e^{i\mathbf{qr}'_\alpha} u_{\alpha c}(\mathbf{r}'_\alpha),$$

$$\sigma^{(\alpha)}_{tt'} = \Omega_\alpha \sum_{k_\alpha} \psi^*_{\alpha vt'}(\mathbf{r}_{k_\alpha}) e^{i\mathbf{qr}_{k_\alpha}} \psi_{\alpha ct}(\mathbf{r}_{k_\alpha}). \tag{6}$$

Making the long-wave approximation $qa \ll 1$ (a is the lattice constant of semiconductor), commonly used to obtain analytical expressions for the eigenvalues and eigenvectors of the electronic subsystem in quantum dots [see, e.g., Eq. (4)], we can decompose $e^{i\mathbf{qr}'_\alpha}$ in a Taylor series and restrict ourselves to the first term that gives a nonzero contribution to the elementary cell volume integral. As a result, we obtain

$$S^{(\alpha)}_{tt'}(\mathbf{q}) = i\sigma^{(\alpha)}_{tt'}(\mathbf{qr}^{(\alpha)}_{vc}), \tag{7}$$

where

$$\mathbf{r}^{(\alpha)}_{vc} = \frac{1}{\Omega_\alpha}\int_{\Omega_\alpha} d^3r'_\alpha u^*_{\alpha v}(\mathbf{r}'_\alpha)\mathbf{r}'_\alpha u_{\alpha c}(\mathbf{r}'_\alpha). \tag{8}$$

The absolute value of $\mathbf{r}^{(\alpha)}_{vc}$ can be expressed using a Kane parameter $P^{(\alpha)}=\hbar^2/m_0\langle S|\partial/\partial z|Z\rangle$ (Ref. 31) as follows:

$$|\mathbf{r}^{(\alpha)}_{vc}| = P^{(\alpha)}/E^{(\alpha)}_g.$$

Here m_0 is the mass of the free electron and $E^{(\alpha)}_g$ is the band gap. Replacing the sum over elementary cells in Eq. (6) with the integral over the volume of a nanocrystal we obtain

$$\sigma^{(\alpha)}_{tt'} = \int d^3r_\alpha \psi^*_{\alpha vt'}(\mathbf{r}_\alpha) e^{i\mathbf{qr}_\alpha} \psi_{\alpha ct}(\mathbf{r}_\alpha). \tag{9}$$

Using Eqs. (7) and (9), matrix element (3) can be expressed as follows:

$$M_{DA} = \frac{e^2}{\varepsilon}\frac{1}{2\pi^2}\int d^3q \frac{e^{i\mathbf{qr}}}{q^2}(\mathbf{qr}^{(D)}_{vc})(\mathbf{qr}^{(A)}_{cv})\sigma^{(D)}_{ii'}\sigma^{(A)*}_{f'f}. \tag{10}$$

In order to further simplify Eq. (9), we use a well-known expansion of a plain wave using spherical harmonics.[32] The spherical symmetry of quantum dots allows us to eliminate the dependence of $\sigma^{(\alpha)}_{tt'}$ on the angular coordinates of vector $\mathbf{q}$. Using the relationship between the integral of the three spherical function and the Clebsch-Gordan coefficients,[32] we transform $\sigma^{(\alpha)}_{tt'}$ to the following expression:

$$\sigma^{(\alpha)}_{tt'}(q) = \frac{2}{R_\alpha^3}\sqrt{\frac{2l_\alpha+1}{2l'_\alpha+1}}\sum_{l=0}^{\infty} i^l(2l+1)C^{l'_\alpha 0}_{l_\alpha 0,l0} C^{l'_\alpha m'_\alpha}_{l_\alpha m_\alpha,l0} \times \int_0^{R_\alpha} dr_\alpha r_\alpha^2 \frac{j_{l_\alpha}(k_{n_\alpha l_\alpha} r_\alpha) j_{l'_\alpha}(k_{n'_\alpha l'_\alpha} r_\alpha)}{j_{l_\alpha+1}(\xi_{n_\alpha l_\alpha}) j_{l'_\alpha+1}(\xi_{n'_\alpha l'_\alpha})} j_l(qr_\alpha), \tag{11}$$

where $k_{n_\alpha l_\alpha}=\xi_{n_\alpha l_\alpha}/R_\alpha$. The product of the Clebch-Gordan coefficients

$$C^{l'_\alpha 0}_{l_\alpha 0,l0} C^{l'_\alpha m'_\alpha}_{l_\alpha m_\alpha,l0} \tag{12}$$

determines the selection rules for the transitions of carriers due to resonant energy transfer,

$$|l_\alpha - l| \le l'_\alpha \le l_\alpha + l,$$

$l_\alpha+l'_\alpha+l=$even number,

$$m_\alpha = m'_\alpha.$$

Now we can carry out an integration over the angular variables in Eq. (10), choosing the z axis of our coordinate system to be codirectional with $\mathbf{r}$. As a result, from Eq. (10) we obtain the following expression:

$$M_{DA} = \frac{e^2}{\varepsilon r^3}[I^{(1)}\mathbf{r}^{(D)}_{vc}\mathbf{r}^{(A)}_{cv} - I^{(2)}3(\mathbf{n}_r\mathbf{r}^{(D)}_{vc})(\mathbf{n}_r\mathbf{r}^{(A)}_{cv})], \tag{13}$$

where

$$I^{(l)} = \left(\frac{1}{3}\right)^{l-1}\frac{2}{\pi}\int_0^\infty dx x^l j_l(x)\sigma^{(D)}_{ii'}(x/r)\sigma^{(A)*}_{f'f}(x/r), \tag{14}$$

$l=1,2$, $x=qr$, and $\mathbf{n}_r$ is the unit vector codirectional with $\mathbf{r}$. In Appendix, the expression of $I^{(l)}$ is presented in terms of Appel hypergeometric functions, allowing the analysis of the selection rules in more detail. As shown in Appendix, $I^{(l)}$ are nonzero when $l_D=l'_D$ and $l_A=l'_A$ simultaneously and also when $l_D+l'_D$ and $l_A+l'_A$ have opposite parities.

In the dipole approximation matrix element (13) is given by

$$M_{DA}^{(\mathrm{dd})} = \frac{e^2}{\varepsilon r^3}\delta_{ii'}\delta_{ff'}[\mathbf{r}_{vc}^{(D)}\mathbf{r}_{cv}^{(A)} - 3(\mathbf{n}_r\mathbf{r}_{vc}^{(D)})(\mathbf{n}_r\mathbf{r}_{cv}^{(A)})], \quad (15)$$

where the Kronecker symbols denote that energy transfer is only possible between those states of the donor and acceptor that can be involved in dipole-allowed interband transitions. It is clear that expression (13) is similar in form to Eq. (15). However, in contrast to Eq. (15), Eq. (13) contains amplitudes $I^{(l)}$ characterizing the contribution of multipole interactions. Furthermore, it follows from Eq. (13) directly that energy transfer is always possible between the states involved in the dipole-forbidden interband optical transitions ($i \neq i'$ and $f \neq f'$).

Our analysis shows that in the case of dipole-allowed interband transitions ($i=i'f=f'$) Eq. (13) leads to Eq. (15) and a r^{-3} law applies regardless of interdot distance. In other words, we obtain $I^{(1)}=I^{(2)}=1$ for any r. This result appears surprising because, according to estimation for atomic systems,[22] the ratio of the matrix elements of dipole-quadrupole $M_{DA}^{(\mathrm{dq})}$ and dipole-dipole $M_{DA}^{(\mathrm{dd})}$ interactions should be similar to $\beta=R_\alpha/r$. In our case, when the donor and acceptor are in close contact, this parameter is $\beta \simeq 1/2$. The coincidence of Eqs. (13) and (15) regardless of distance is most likely to be a result of the spherical symmetry of the quantum dots.

A further symmetry that is reflected in our results is a similarity of the envelope wave functions of the electrons in the conduction and valence bands obtained using a two-band approximation. In this case, the envelope wave functions do not contain any band-specific parameters and are mutually orthonormal. Clearly, if the degeneration of the valence band and mixing of its subbands are taken into account, this symmetry will be broken. For a complex valence-band structure the wave functions of the holes are described by linear combinations of expressions of the form $C_\varkappa j(k_\varkappa r)Y_{JM}(\theta,\phi)$. Here, $C_\varkappa$ are coefficients that depend on the band parameters and J and M are the total momentum and its projection.[33] The interdot matrix element will now have a more complex form and Eq. (13) does not coincide with Eq. (15) even for dipole-allowed transitions.

As can be seen from Eq. (13), the probability of energy transfer depends on the square of the orientational factor given by

$$\chi(\theta_D,\theta_A,\phi) = \sin\,\theta_D \sin\,\theta_A \cos\,\phi - 2\cos\,\theta_D \cos\,\theta_A. \quad (16)$$

This factor defines the mutual orientations of the dipole moments of the interband transitions and the vector $\mathbf{r}$. This means that the energy transfer is essentially anisotropic. We use a spherical coordinate system where z axis is parallel to $\mathbf{r}$, θ_D and θ_A are the polar angles of the dipole moments of the donor and acceptor, respectively, and ϕ is the difference between their azimuth angles. Equation (16) shows that χ^2 takes values from 0 to 4 and so has a substantial impact on the effectiveness of energy transfer.

Now, we calculate the orientations of the dipole moments that lead to maximum and minimum values for χ^2. The surfaces of constant χ^2 are given by the following expression:

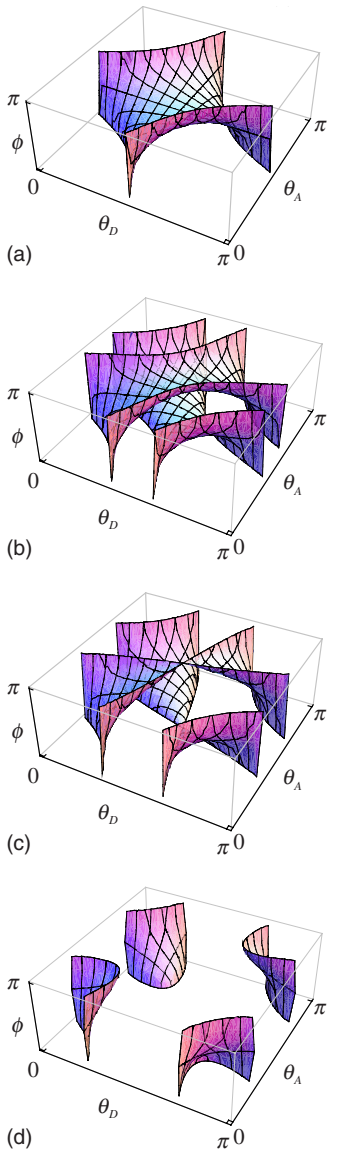

FIG. 3. (Color online) Surfaces of constant χ^2: (a) $\chi^2=0$, (b) $\chi^2=0.5$, (c) $\chi^2=1$, and (d) $\chi^2=2$.

$$\phi = \arccos\left(\frac{\pm\chi + 2\cos\,\theta_D \cos\,\theta_A}{\sin\,\theta_D \sin\,\theta_A}\right).$$

Figure 3 shows plots of these surfaces for various values of χ^2. From Fig. 3 it is clear that for any given values of θ_D and θ_A there is a corresponding ϕ that gives $\chi^2=0$.

When one of the dipole moments is parallel to $\mathbf{r}$ ($\theta_\alpha=0$ or π) we have

$$\chi^2 = 4\cos^2\,\theta_\beta,$$

i.e., Eq. (16) no longer depends on ϕ, and χ^2 is fully determined by the polar angle of the other dipole. In particular, when the second dipole is parallel to the first one ($\theta_\beta=0$ or π), χ^2 is the maximum value $\chi^2_{\max}=4$. Thus, maximum energy-transfer efficiency is achieved at the following dipole moment orientations: (1) $\theta_D=0$, $\theta_A=0$; (2) $\theta_D=0$, $\theta_A=\pi$; (3) $\theta_D=\pi$, $\theta_A=0$; and (4) $\theta_D=\pi$, $\theta_A=\pi$.

This anisotropy offers the possibility of creating a photoexcitation energy transmission line between the spatially separated points. Indeed, if we construct a chain of quantum dots with suitable sizes and parallel interband transition dipole moments, we can obtain an effective energy "conductor." Conversely, if the orientation of the dipole moments corresponds to the case $\chi^2=0$ depicted in Fig. 3(a), then we will have an effective "insulator" for the photoexcitation energy. A combination of these two cases allows the construction of networks with a variety of architectures for controlled transport of photoexcitation energy in close-packed quantum dot systems.

For the sake of simplicity, in subsequent discussions we consider the probability of energy transfer averaged over the directions of the dipole moments of the interband transitions. If the donor and acceptor are made from the same material, the square modulus of matrix element (13), averaged over all dipole moment directions for the interband transitions, will be equal to

$$\overline{|M_{DA}|^2} = \frac{1}{3}\frac{e^4}{\varepsilon^2 r^6}\left(\frac{P}{E_g}\right)^4 \{|I^{(1)}|^2 - (I^{(1)*}I^{(2)} + I^{(1)}I^{(2)*}) + 3|I^{(2)}|^2\}. \tag{17}$$

For the dipole-dipole approximation or for the dipole-allowed interband transitions, this can be written as

$$\overline{|M_{DA}^{(\mathrm{dd})}|^2} = \frac{2}{3}\frac{e^4}{\varepsilon^2 r^6}\left(\frac{P}{E_g}\right)^4 \delta_{n_D n'_D}\delta_{n_A n'_A}\delta_{l_D l'_D}\delta_{l_A l'_A}\delta_{m_D m'_D}\delta_{m_A m'_A}.$$

Let us consider this matrix element for a specific case, namely, for the lowest energy transitions when the matrix element is nonzero. We assume that initially the electron and hole are in the lowest energy states $i=i'=\{100\}$. This case is of particular interest when the rate of intraband relaxation of carriers is much higher than that of energy transfer. We shall consider quantum dots formed from the cubic modification of CdSe (Ref. 34): $m_c^{(\alpha)}=0.11m_0$, $m_v^{(\alpha)}=1.14m_0$, $E_g^{(\alpha)}(293\ \mathrm{K})=1.736$ eV, $P=1.48\times10^{-19}$ cm^3 g s^{-2}, and $\varepsilon_\alpha=5.8$, embedded in an SiO_2 matrix with a high-frequency dielectric constant $\varepsilon_M=2.13$.[35] From Eq. (2) we have the effective dielectric constant $\varepsilon=5.28$. Obviously, the rate of energy transfer will be maximum when the transition energies in the donor and acceptor are equal. In our case (see Fig. 4) this condition is satisfied when radii R_D and R_A are coupled by the following expression:

$$\frac{R_D}{R_A} = \pi\sqrt{\frac{m_c+m_v}{m_c\xi_{nl}^2 + m_v\xi_{n'l'}^2}}, \tag{18}$$

where n,l and n',l' are the quantum numbers of the states in the valence and conduction bands of the acceptor. Figure 5 shows the dependence of $\overline{|M_{DA}|^2}$ on the distance between the centers of the quantum dots in the cases of resonance with various transitions in the acceptor: dipole-allowed transitions $Av\{nlm\}\rightarrow Ac\{nlm\}$ and dipole-forbidden transitions $Av\{110\}\rightarrow Ac\{120\}$, $Av\{120\}\rightarrow Ac\{110\}$, $Av\{100\}\rightarrow Ac\{110\}$, $Av\{110\}\rightarrow Ac\{100\}$. In our calculations, we assume that the donor radius $R_D=2$ nm and the acceptor radius are chosen to satisfy Eq. (18), ensuring resonance. From Fig. 5 it is clear that the relative magnitude of the square of the modulus of the matrix element for dipole-forbidden transitions can be up to ~20% of the corresponding value for dipole-allowed transition at short interdot distances. Since energy transfer involving the dipole-forbidden transitions of the acceptor is caused by the multipole, including quadrupole, interactions, these results agree with the initial estimate of 25% for the relative contribution of quadrupole interactions to the energy transfer made in Sec. I.

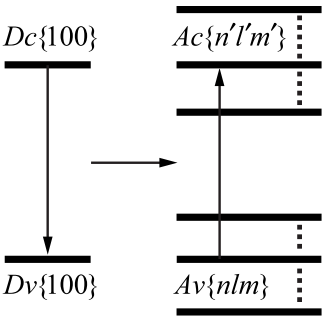

FIG. 4. Schematic diagram depicting the resonant transfer of electronic excitation energy from a quantum dot donor to a quantum dot acceptor. The lowest energy interband transition in a donor ($Dc\{100\}\rightarrow Dv\{100\}$) and the corresponding resonant interband transition in an acceptor ($Av\{nlm\}\rightarrow Ac\{n'l'm'\}$) are shown.

Some remarks on generalizing these results to the case of quantum dots with finite potential walls are appropriate at this point. In this case, dipole-allowed interband transitions can occur between states with different principal quantum numbers, e.g., when $n_\alpha \neq n'_\alpha$. This is because envelope functions depend on the band parameters of semiconductors and the depth of the potential well.[36] As a result, the radial parts of the envelope functions of electrons $R_{\alpha c n_\alpha l_\alpha}(r_\alpha)$ and holes $R_{\alpha v n'_\alpha l_\alpha}(r_\alpha)$ are not orthonormal,

$$G_{cn_\alpha,vn'_\alpha} = \int_0^\infty dr_\alpha r_\alpha^2 R_{\alpha c n_\alpha l_\alpha}(r_\alpha) R_{\alpha v n'_\alpha l_\alpha}(r_\alpha) \neq 0.$$

Note that all other properties of the energy-transfer-matrix element related to the angular parts of envelope functions remain the same. Thus, if we replace

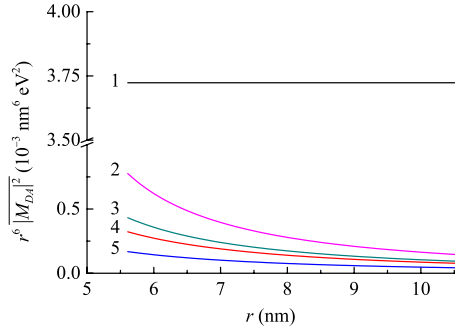

FIG. 5. (Color online) Dependence of the square of the modulus of the energy-transfer-matrix element on the distances between the centers of the donor and acceptor. (1) $Av\{nlm\}\rightarrow Ac\{nlm\}$, (2) $Av\{110\}\rightarrow Ac\{120\}$, (3) $Av\{120\}\rightarrow Ac\{110\}$, (4) $Av\{100\}\rightarrow Ac\{110\}$, and (5) $Av\{110\}\rightarrow Ac\{100\}$.

$$\frac{2}{R_\alpha^3}\frac{j_{l_\alpha}(k_{n_\alpha l_\alpha} r_\alpha) j_{l'_\alpha}(k_{n'_\alpha l'_\alpha} r_\alpha)}{j_{l_\alpha+1}(\xi_{n_\alpha l_\alpha}) j_{l'_\alpha+1}(\xi_{n'_\alpha l'_\alpha})}$$

by $R_{\alpha c n_\alpha l_\alpha}(r_\alpha) R_{\alpha v n'_\alpha l'_\alpha}(r_\alpha)$ in Eqs. (11) and (A3) and replace the upper limits of integration over r_D and r_A in Eqs. (11) and (A1) by infinity, we obtain expressions applicable for quantum dots with finite potential walls. In particular, the matrix element of energy transfer for dipole-allowed interband transitions will be equal to

$$M_{DA}^{(\mathrm{dd})} = \frac{e^2}{\varepsilon r^3} G_{cn_D, vn'_D} G_{cn_A, vn'_A} \delta_{l_D l'_D} \delta_{l_A l'_A} \delta_{m_D m'_D} \delta_{m_A m'_A} \times [\mathbf{r}_{vc}^{(D)} \mathbf{r}_{cv}^{(A)} - 3(\mathbf{n}_r \mathbf{r}_{vc}^{(D)})(\mathbf{n}_r \mathbf{r}_{cv}^{(A)})].$$

III. ENERGY-TRANSFER RATE

Using Eq. (17), it is possible to calculate the rate of resonant energy transfer from any fixed donor state to all possible acceptor states γ_{DA}. Because the interaction of the charge carriers of the donor and acceptor is weak, we can use first-order perturbation theory to describe the probability of energy transfer from electron-hole pairs of the donor in state $|i_D, i'_D\rangle$ to electron-hole pairs of the acceptor in state $|f_A, f'_A\rangle$. We obtain the following expression for the rate of resonant energy transfer:

$$\gamma_{DA} = \frac{2}{\hbar^2} \overline{|M_{DA}|^2} \frac{\Gamma_{DA}}{\Gamma_{DA}^2 + \Delta_{DA}^2},$$

where

$$\Delta_{DA} = (E_{c,i}^{(D)} + E_{v,i'}^{(D)} + E_g^{(D)} - E_{c,f'}^{(A)} - E_{v,f}^{(A)} - E_g^{(A)})/\hbar.$$

Here, Δ_{DA} is the detuning between the frequencies of the electron-hole pair transitions in the donor and acceptor involved in the energy-transfer process, $E_{\varkappa,t}^{(\alpha)} = \hbar^2 \xi_{n_\alpha l_\alpha}^2 / (2 m_\varkappa^{(\alpha)} R_\alpha^2)$, and Γ_{DA} is the coherence relaxation rate between the initial and final states. For the case of dipole-allowed transitions, the rate of energy transfer from the donor state with quantum numbers n_D, l_D, m_D to all possible acceptor states is given by

$$\gamma_{DA}^{(\mathrm{dd})} = \frac{4e^4}{3\hbar^2 \varepsilon^2 r^6} \left(\frac{P}{E_g}\right)^4 \sum_{n_A l_A} (2l_A + 1) \frac{\Gamma_{DA}}{\Gamma_{DA}^2 + \Delta_{DA}^2}.$$

The summation is performed over all possible acceptor states. We define Γ_{DA} as the sum of the dephasing rates of interband transitions in the donor and acceptor,

$$\Gamma_{DA} = \gamma_{i'_D i_D} + \gamma_{f'_A f_A}, \tag{19}$$

where $\gamma_{t't} = (\gamma_{t'} + \gamma_t)/2 + \bar{\gamma}_{t't}$, γ_t is the reciprocal lifetime of state t in the donor or acceptor, and $\bar{\gamma}_{t't}$ is the pure dephasing rate of the transition. Hence, the rate of energy transfer is expected to have a significant temperature dependence, in agreement with experimental data.[4] The finite width of the transitions involved in the energy transfer results in several important consequences. First, exact resonance between the donor and acceptor levels is not required for the transfer of electronic excitation energy. In order to illustrate this statement, consider the example of a transition between the dipole-allowed states of a CdSe quantum dot donor and acceptor $Dc\{100\}, Dv\{100\} \rightarrow Av\{11m\}, Ac\{11m\}$. Figure 6 shows the dependence of the energy-transfer rate γ_{DA} on energy detuning between the energies of electron-hole pair transitions in the donor and acceptor at both room temperature and liquid-helium temperature. In this calculation we use a phenomenological equation for the dephasing rate of the interband transitions which is frequently used for the analysis of experimental data,[37,38]

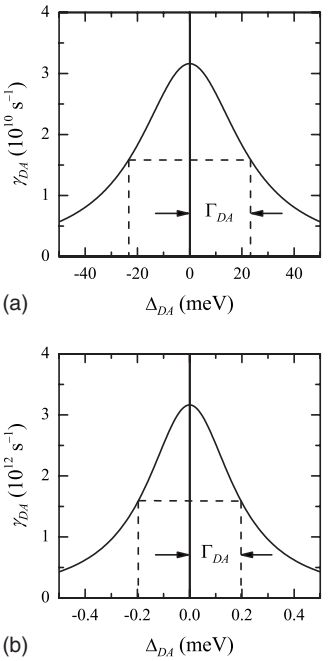

FIG. 6. Rate of energy transfer γ_{DA} for CdSe quantum dots as a function of energy detuning Δ_{DA}. The interdot distance is $r = 5$ nm; Γ_{DA} is the transition dephasing rate [Eq. (19)] expressed as an energy. (a) $T = 300$ K and (b) $T = 4$ K.

$$\gamma_{cv} = \gamma_0 + aT + b\bar{n}_{\mathrm{LO}}(T), \tag{20}$$

where $\bar{n}_{\mathrm{LO}}(T) = 1/[\exp(\hbar\omega_{\mathrm{LO}}/k_B T) - 1]$, ω_{LO} is the frequency of the longitudinal optical (LO) phonon in the donor or acceptor, k_B is the Boltzmann constant, and T is the temperature. In Eq. (20), the first term γ_0 is interpreted as a dephasing rate due to both nonradiative and radiative interband transitions. The second and third terms describe the interaction with acoustic and optical phonons ($a = 1.5 \times 10^{10}$ s^{-1}/K,[37,38] $b = 2.3 \times 10^{13}$ s^{-1},[37] and $\hbar\omega_{\mathrm{LO}} = 26$ meV). For a donor in the lowest excited state a γ_0 value of 7.7×10^7 s^{-1} was chosen, corresponding to a quantum yield of 50% and a radiative transition width of nearly 3.85×10^7 s^{-1}.[39] For an acceptor in a highly excited state we should consider the contribution from intraband relaxation of electron-hole pairs to γ_0. According to paper,[40] the intraband relaxation rate for transitions between the lowest energy states of electron-hole pairs in CdSe quantum dots varies from 10^{11} to 3.3×10^{12} s^{-1} when quantum dot radius reduces from 5.6 to 2 nm. In our calculations (Fig. 6), a value of 2

$\times 10^{11}$ s^{-1} for the contribution of intraband relaxation to γ_0 has been chosen. Figure 6 clearly shows that, within the width of Γ_{DA}, effective energy transfer is possible with both raising and lowering of the transition energy. With decreasing temperature [Fig. 6(b)] the probability of the energy transfer increases significantly, and the transition width decreases. At room temperature [Fig. 6(a)] it is possible to have a situation where several energy levels of the acceptor are within the spectral range of $-\Gamma_{DA} \leq \Delta_{DA} \leq \Gamma_{DA}$. In this case, an effective energy transfer to all these levels will take place. It should be emphasized that utilization of Eq. (20) with the values of parameters γ_0, a, b, and $\hbar\omega_{\mathrm{LO}}$ mentioned is equivalent to using of experimental data.

It is necessary to make several remarks regarding Eq. (20). In spite of the fact that it is used by many authors for the analysis of experimental data on the temperature dependence of the excitonic and interband transition dephasing rate, its application to quantum dots is not entirely physically justified. Originally Eq. (20) was proposed for description of the dephasing of excitonic optical transitions to the lowest energy state (exciton wave vector $\mathbf{K}=0$) in bulk semiconductors,[41,42] whose electronic subsystem has a continuous energy spectrum. This equation remains valid for the interband transitions in bulk materials. Interpretation of the three terms in Eq. (20) in these cases is clear: the first one describes pure dephasing due to scattering by impurities and defects, the natural transition width, and possible nonradiative exciton recombination; the second and third terms describe dephasing due to real transitions with the absorption of acoustic and LO phonons, respectively, which is always possible in systems with a continuous energy spectrum. Processes with the absorption of transversal optic (TO) phonons are neglected in Eq. (20) because in A_2B_4 and A_3B_5 semiconductors, interaction with LO phonons is dominating.

For describing the dephasing of excitonic and interband optical transitions to an energy state different from the lowest one we must modify Eq. (20). If the energy of an excited electron-hole pair is larger than the lowest energy of the pair by the value E, with E greater than the acoustic or optical phonon energies, the expression for the temperature dependence of the dephasing rate of the interband transition contains one or two additional terms. If $0<E<\hbar\omega_{\mathrm{LO}}$, then we obtain an additional term a_1T, similar in form to aT in Eq. (20), but describing the emission of an acoustic phonon. If $\hbar\omega_{\mathrm{LO}}<E$, a second additional term $b_1[\bar{n}_{\mathrm{LO}}(T)+1]$ will appear describing emission of the LO phonon. Thus, generalization of Eq. (20) to the case of dephasing of the high energy excitonic and interband transition in semiconductors is given by the equation

$$\gamma_{cv} = \gamma_0 + \bar{a}T + b\bar{n}_{\mathrm{LO}}(T) + \begin{cases} 0, & 0 < E < \hbar\omega_{\mathrm{LO}} \\ b_1[\bar{n}_{\mathrm{LO}}(T)+1], & \hbar\omega_{\mathrm{LO}} < E, \end{cases} \tag{21}$$

where $\bar{a}=a+a_1$. Equation (21) is valid for structures with a continuous energy spectrum, such as bulk semiconductors, quantum wells, and quantum wires. It should be pointed out that in Eq. (21) we do not consider processes that lead to pure dephasing of interband transitions due to phonon scattering. The contributions of these processes to γ_{cv} in the case of weak electron-phonon interaction[43] are $b_{\mathrm{pd}}\bar{n}_{\mathrm{LO}}(T)[\bar{n}_{\mathrm{LO}}(T)+1]$ for LO-phonon scattering and $a_{\mathrm{pd}}T^2$ for acoustic phonon scattering. The linear $\bar{a}T$ and quadratic $a_{\mathrm{pd}}T^2$ dependencies that appear due to interaction with acoustic phonons are valid when $T \gg 1$ K, i.e., for when the acoustic mode population is large.[31] If this condition is not met, then the contribution from pure dephasing due to acoustic phonon scattering to γ_{cv} will be proportional to T^7 (Refs. 1 and 43). In any case, when $T \to 0$ K, pure dephasing due to phonon scattering does not occur. If pure dephasing due to phonon scattering is taken into account, the following expression is obtained for γ_{cv}:

$$\gamma_{cv} = \gamma_0 + \bar{a}T + b\bar{n}_{\mathrm{LO}}(T) + a_{\mathrm{pd}}T^2 + b_{\mathrm{pd}}\bar{n}_{\mathrm{LO}}(T)[\bar{n}_{\mathrm{LO}}(T)+1] + \begin{cases} 0, & 0 < E < \hbar\omega_{\mathrm{LO}} \\ b_1[\bar{n}_{\mathrm{LO}}(T)+1], & E > \hbar\omega_{\mathrm{LO}}. \end{cases} \tag{22}$$

This equation is not generally applicable, since it does not include the contributions from interactions with elementary excitations within semiconductor structure, such as TO phonons, plasmons, plasmon-phonon modes, and magnons, as well as contributions from tunneling and activation processes leading to trapping and releasing of carriers. The contribution from activation processes to γ_{cv} is described, in general, by expressions of the type $c_a \exp(-E_a/k_BT)$, where E_a is the activation energy.

Let us consider the validity of Eq. (22) for the description of transition dephasing in semiconductor quantum dots whose electronic subsystem has a discrete energy spectrum. Clearly, in this case, γ_{cv} should always contain the first, fourth, and fifth terms. However, the interpretation of γ_0 is somewhat altered. In contrast to bulk material, quantum wells, and wires, whose charge carriers and excitons are represented by running waves, electronic excitations of this type in quantum dots are standing waves. Therefore, the concept of electron scattering on defects and impurities loses physical meaning. Thus, for quantum dots, γ_0 is determined by the natural transition width and the nonradiative recombination of electron-hole pairs or excitons. The contribution to γ_{cv} from processes of pure dephasing, as described by the fourth and fifth terms of Eq. (22), remains because pure dephasing does not change the population of the electronic levels and does not require a continuous electronic spectrum. The second, third, and sixth terms of Eq. (22) describing contributions from real transitions between the levels of the electronic subsystem are more complex to describe. These terms only appear when the energy gaps between the electronic (excitonic) states are sufficiently close to the energies of acoustic or optical phonons. In order to describe this in detail, we use the example of dipole-allowed interband transitions to the lowest energy state, E_0, of the electron-hole pair. In this instance, the sixth term of Eq. (22) is absent because there are no states with energy $E_{\mathrm{low}}<E_0$ in the quantum dot. Dephasing associated with the transition to the higher energy state $E_{\mathrm{high}}>E_0$ with optical phonon absorption [third term in Eq. (22)] can take place only if $E_{\mathrm{high}}-E_0 \approx \hbar\omega_{\mathrm{LO}}$. This is possible only for quantum dots of a specific size. Therefore, the presence and value of the third term in Eq. (22) is determined by the following parameters characterizing the quan-

tum dots: size, shape, depth of potential well, effective masses of carriers, and others. Thus, the contribution from dephasing processes of this type to γ_{cv} is not universal.

Finally, let us discuss the second term of Eq. (22), corresponding to real transitions between levels of electron-hole pairs involving acoustic phonons. At present, it is known that the fundamental interband transition within quantum dots has a fine structure. If exchange interaction is neglected, then the lowest energy state of the electron-hole pairs is eightfold degenerated in semiconductors with cubic symmetry and fourfold degenerated in materials with hexagonal symmetry. Exchange interaction partially removes this degeneration. Lowering of the symmetry due to shape of quantum dot also removes degeneration. Thus, fine structure of the energy spectrum of electron-hole pairs with a characteristic energy scale of a few meV appears.[44–46] Transitions between components of this fine structure with the absorption and emission of acoustic phonons cause an increase in the second term in Eq. (22). As a result, we obtain the following expression for the dephasing rate of interband transitions to the lowest energy state in a quantum dot:

$$\gamma_{cv} = \gamma_0 + \bar{a}T + b\bar{n}_{\mathrm{LO}}(T) + a_{\mathrm{pd}}T^2 + b_{\mathrm{pd}}\bar{n}_{\mathrm{LO}}(T)[\bar{n}_{\mathrm{LO}}(T) + 1]. \tag{23}$$

This equation differs from Eq. (20) by the presence of the last two terms. Evidently, different dephasing mechanisms will dominate over different temperature ranges, quantum dot materials, and geometries. Consequently, determination of the contributions of different dephasing sources is difficult. Indeed, let us consider third and fifth terms in Eq. (23) which are responsible for the interaction of the electronic subsystem with optical phonons. In the majority of A_2B_4 and A_3B_5 materials the optical phonon energy is in the range between 20 and 40 meV.[47] Therefore, in the range $0 < T \leq 150$ K the temperature dependence of both terms will have a similar form $\exp(-\hbar\omega_{\mathrm{LO}}/k_BT)$, and it is impossible to distinguish their individual contributions to γ_{cv}. In conclusion, the problem of experimental identifying the dominant dephasing mechanisms of the interband transitions at temperatures $T > 50$ K remains open.

The analysis presented above shows that temperature is a crucial parameter in determining, in many cases, the efficiency of energy transfer. This originates in the temperature dependence of the coherence relaxation rate Γ_{DA} between the initial and final states of the energy-transfer process.

IV. PHOTOLUMINESCENCE SPECTRUM

Let us consider the luminescence of donors and acceptors taking into account nonradiative resonant energy transfer. For this purpose we use a reduced density-matrix formalism, adapted for the calculation of secondary emission from quantum dots.[48]

The Hamiltonian of donor and acceptor quantum dots, interacting with an external optical field and the quantum electromagnetic field of the vacuum has the following form:

$$H = H_D + H_A + H_R + H_{DR} + H_{DL} + H_{AR} + H_{AL},$$

where

$$H_\alpha = \sum_{i_\alpha} \hbar\omega_{i_\alpha} |i_\alpha\rangle\langle i_\alpha|$$

are the Hamiltonians of noninteracting electron-hole pairs in the donor ($\alpha = D$) and acceptor ($\alpha = A$) in terms of their eigenvectors $|i_\alpha\rangle$ and eigenvalues $\hbar\omega_{i_\alpha}$. In the case of a strong confinement and spherical quantum dots $\hbar\omega_{i_\alpha} = E_g^{(\alpha)} + \hbar^2\xi^2_{n_\alpha l_\alpha}/(2m_c^{(\alpha)}R_\alpha^2) + \hbar^2\xi^2_{n'_\alpha l'_\alpha}/(2m_v^{(\alpha)}R_\alpha^2)$.

$$H_R = \sum_k \hbar\omega_k b_k^+ b_k$$

is the Hamiltonian of electromagnetic field, b_k^+ and b_k are the operators of creation and annihilation of photons in the state k with frequency ω_k.

$$H_{\alpha R} = i\hbar \sum_{i_\alpha, k} \rho_{\alpha k}(V^{(k)}_{i_\alpha g_\alpha} b_k |i_\alpha\rangle\langle g_\alpha| - \text{c.c.}),$$

$$H_{\alpha L} = \frac{1}{2}\sum_{i_\alpha} [\phi(t) V^{(L)}_{i_\alpha g} e^{-i\omega_L t} |i_\alpha\rangle\langle g_\alpha| + \text{c.c.}]$$

are the operators describing the interaction of donor and acceptor electron-hole pairs with the quantum electromagnetic field and external classical optical field with frequency ω_L, $|g_\alpha\rangle$ is the vacuum state of the electron-hole pairs, $\rho_{\alpha k} = \sqrt{2\pi\omega_k/\varepsilon_\alpha\hbar V}$, ε_α is the dielectric constant of the corresponding quantum dot, V is the normalization volume, $V_{if}^{(\eta)} = \langle i|(-e\mathbf{r})\mathbf{e}_\eta|f\rangle$, $\eta = L, k$, $e\mathbf{r}$ is the dipole moment operator, $\mathbf{e}_\eta$ is the polarization vector of the photon, and $\phi(t)$ is the complex amplitude of the electromagnetic filed.

The evolution of the states of noninteracting quantum dots can be described by kinetic equations for reduced density matrices,

$$\dot{\rho}^{(\alpha)}_{f'_\alpha f_\alpha} = \frac{1}{i\hbar}[H, \rho^{(\alpha)}]_{f'_\alpha f_\alpha} + \delta_{f'_\alpha f_\alpha} \sum_{f''_\alpha \neq f_\alpha} \zeta_{f_\alpha f''_\alpha} \rho^{(\alpha)}_{f''_\alpha f''_\alpha} - \gamma^{(0)}_{f'_\alpha f_\alpha} \rho^{(\alpha)}_{f'_\alpha f_\alpha}, \tag{24}$$

where $\gamma^{(0)}_{f_\alpha f_\alpha}$ is the population relaxation rate of state f_α, proportional to the reciprocal of its lifetime, $\gamma^{(0)}_{f'_\alpha f_\alpha} = (\gamma^{(0)}_{f'_\alpha f'_\alpha} + \gamma^{(0)}_{f_\alpha f_\alpha})/2 + \bar{\gamma}^{(0)}_{f'_\alpha f_\alpha}$ for $f'_\alpha \neq f_\alpha$ is the coherence relaxation rate, $\bar{\gamma}^{(0)}_{f'_\alpha f_\alpha} = \bar{\gamma}^{(0)}_{f_\alpha f'_\alpha}$ is the pure dephasing rate, and $\zeta_{f'_\alpha f_\alpha}$ is the rate of transition from f_α to f'_α.

We will take a phenomenological approach to describing the interaction between the donor and acceptor using the expression for the rate of energy transfer γ_{DA} obtained in Sec. III. Interaction of the quantum dots leads to several changes in the system of Eq. (24). In the equations describing the population evolution, additional terms related to the creation and annihilation of electron-hole pairs in the donor and acceptor due to energy transfer will appear. Thus, instead of two independent systems for the donor and acceptor one system of coupled equations arises. Furthermore, in the equations describing the evolution of coherence for the states involved in the energy-transfer process, we redefine the coherence relaxation rates: $\gamma^{(0)}_{f'_\alpha f_\alpha} \to \gamma_{f'_\alpha f_\alpha} = \gamma^{(0)}_{f'_\alpha f_\alpha} + \gamma_{DA}/2$.

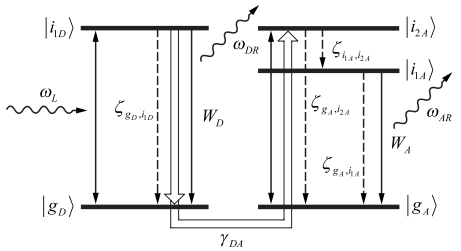

FIG. 7. Schematic diagram depicting transitions in a system of two interacting quantum dots (donor and acceptor). Solid lines show transitions leading to absorption or emission of photons with frequencies ω_L and $\omega_{\alpha R}$; dotted lines show transitions with rates $\zeta_{f_\alpha f'_\alpha}$ caused by thermal bath interaction.

In order to further illustrate this, consider the following diagram depicting the luminescence of donors and acceptors (Fig. 7). A monochromatic light wave with field strength E_L and frequency ω_L resonantly excites the donor to the dipole-allowed lowest energy state $|i_{1D}\rangle$. The external excitation is also in resonance with the state $|i_{2A}\rangle$ of the acceptor. There are two distinct cases, since optical transition to this state of the acceptor is either allowed or forbidden. In the second case we can neglect interaction with the external emission. We assume that the radiative recombination rate of state $|i_{2A}\rangle$ is much smaller than the rate intraband relaxation. So, we can neglect secondary emission of the acceptor at the frequency of $|g_A\rangle \rightarrow |i_{2A}\rangle$ transition. The donor has three relaxation channels to the ground state: (1) nonradiative recombination due to thermal bath interaction, (2) radiative recombination with an associated emission of a photon at a frequency ω_{DR}, and (3) nonradiative recombination with energy transfer to the acceptor (transition $|i_{1D}\rangle \rightarrow |i_{2A}\rangle$). These channels are characterized by rates $\zeta_{g_Di_{1D}}$, W_D, and γ_{DA}, respectively. We assume that the intraband relaxation rate of carriers is much larger than the energy-transfer rate and the interband recombination rate, that is, the following condition is satisfied,

$$\zeta_{i_{1A},i_{2A}} \gg \gamma_{DA}, \zeta_{g_\alpha,i_{1\alpha}},$$

and the acceptor quickly relaxes to the lowest excited state $|i_{1A}\rangle$, which is dipole allowed for optical transitions. The condition $\zeta_{i_{1A}i_{2A}} \gg \gamma_{DA}$ also guarantees that there is no reverse energy-transfer process from acceptor to donor.

Depending on the mechanism of intraband relaxation considered,[49–51] the value of relaxation rate can vary from 10^{11} to 10^{12} s^{-1}. The analysis of the energy-transfer rate performed in Sec. III showed that γ_{DA} is about 10^{10} s^{-1} at room temperature [Fig. 6(a)]. Therefore, the condition $\zeta_{i_{1A}i_{2A}} \gg \gamma_{DA}$ is obeyed. At low temperatures, liquid-helium temperature, for example, $\gamma_{DA} \sim 10^{12}$ s^{-1} [Fig. 6(b)], i.e., the condition $\zeta_{i_{1A}i_{2A}} \gg \gamma_{DA}$ is not satisfied. Now, reverse energy transfer from acceptor to donor must be considered. This case will be comprehensively investigated in future work. In the present study, we restrict ourselves to consideration of the room-temperature case.

Finally, transitions can occur from acceptor state $|i_{1A}\rangle$ to the ground state due to thermal bath interaction and also due to electron-hole recombination with photon emission at a frequency ω_{AR}. These processes are characterized by rates $\zeta_{g_Ai_{1A}}$ and W_A, respectively.

In order to describe the luminescence we use the following simplified electron-photon system:

$$|1\rangle_D = |g_D\rangle|g_A\rangle|0_k\rangle, \quad |2\rangle_D = |i_{1D}\rangle|g_A\rangle|0_k\rangle,$$

$$|3\rangle_D = |g_D\rangle|g_A\rangle|1_{Dk}\rangle,$$

$$|1\rangle_A = |g_A\rangle|g_D\rangle|0_k\rangle, \quad |2\rangle_A = |i_{1A}\rangle|g_D\rangle|0_k\rangle,$$

$$|3\rangle_A = |i_{2A}\rangle|g_D\rangle|0_k\rangle, \quad |4\rangle_A = |g_A\rangle|g_D\rangle|1_{Ak}\rangle,$$

where $|0_k\rangle$ is the vacuum of photons emitted by quantum dots and $|1_{Dk}\rangle$ and $|1_{Ak}\rangle$ are the states with one photon emitted by the donor and acceptor, respectively. This system is applicable when the excitation light is of low intensity, the saturation of the optical transitions can be neglected, and multiphoton processes of excitation and radiation are ignored.

Using this system, together with modified kinetic equation [Eq. (24)], and the condition $\zeta_{i_{1A}i_{2A}} \gg \gamma_{DA}$, we can write the system of equations for the populations of the donor and acceptor states in the following forms:

$$\dot{\rho}_{11}^{(D)} = \frac{1}{i\hbar}[H,\rho^{(D)}]_{11} + \gamma_{i_{1D}i_{1D}}\rho_{22}^{(D)},$$

$$\dot{\rho}_{22}^{(D)} = \frac{1}{i\hbar}[H,\rho^{(D)}]_{22} - \gamma_{i_{1D}i_{1D}}\rho_{22}^{(D)},$$

$$\dot{\rho}_{33}^{(D)} = \frac{1}{i\hbar}[H,\rho^{(D)}]_{33}, \tag{25}$$

$$\dot{\rho}_{11}^{(A)} = \frac{1}{i\hbar}[H,\rho^{(A)}]_{11} + \gamma_{i_{1A}i_{1A}}^{(0)}\rho_{22}^{(A)} + \zeta_{g_Ai_{2A}}\rho_{33}^{(A)} - \gamma_{DA}\rho_{22}^{(D)},$$

$$\dot{\rho}_{22}^{(A)} = \frac{1}{i\hbar}[H,\rho^{(A)}]_{22} - \gamma_{i_{1A}i_{1A}}^{(0)}\rho_{22}^{(A)} + \zeta_{i_{1A}i_{2A}}\rho_{33}^{(A)},$$

$$\dot{\rho}_{33}^{(A)} = \frac{1}{i\hbar}[H,\rho^{(A)}]_{33} - \gamma_{i_{2A}i_{2A}}^{(0)}\rho_{33}^{(A)} + \gamma_{DA}\rho_{22}^{(D)},$$

$$\dot{\rho}_{44}^{(A)} = \frac{1}{i\hbar}[H,\rho^{(A)}]_{44}, \tag{26}$$

where (see Fig. 7)

$$\gamma_{i_{1D}i_{1D}} = \gamma_{i_{1D}i_{1D}}^{(0)} + \gamma_{DA} = \zeta_{g_Di_{1D}} + \gamma_{DA},$$

$$\gamma_{i_{2A}i_{2A}}^{(0)} = \zeta_{i_{1A}i_{2A}} + \zeta_{g_Ai_{2A}}, \gamma_{i_{1A}i_{1A}}^{(0)} = \zeta_{g_Ai_{1A}}.$$

It is clear from Eqs. (25) and (26) that population is conserved not only for the system as a whole but also for the donor and acceptor separately,

$$\sum_{n=1}^{3} \dot{\rho}^{D}_{nn} = 0, \quad \sum_{n=1}^{4} \dot{\rho}^{A}_{nn} = 0,$$

i.e., there is no charge transfer in the donor/acceptor system.

Considering a stationary external excitation $[\phi(t)=E_L]$ and using Eqs. (25) and (26) and a system of modified equations for the nondiagonal elements of the density matrix [Eq. (24)], one can obtain the luminescence differential cross section (LDCS) per unit solid angle Θ and per unit of frequency $\omega_{\alpha R}$. LDCS is related to the photon emission rates $W_D=\dot{\rho}^{D}_{33}$ and $W_A=\dot{\rho}^{A}_{44}$ by the following expression:

$$\frac{d^2\sigma_\alpha}{d\Theta d\omega_{\alpha R}} = \frac{V\hbar\omega^3_{\alpha R}}{4(\pi c)^3}\frac{W_\alpha(\omega_{\alpha R})}{I_L},$$

where I_L is the intensity of the exciting light wave. Performing a calculation in the lowest order of perturbation theory by interaction with the external classical optical field and with the quantum electromagnetic field of the vacuum, one obtains the following expression for the differential cross section of the donor luminescence:

$$\frac{d^2\sigma_D}{d\Theta d\omega_{DR}} = C(\omega_{DR})|V^{(R)}_{g_D i_{1D}}|^2|V^{(L)}_{i_{1D}g_D}|^2 \times \frac{\bar{\gamma}^{(0)}_{g_D i_{1D}}}{\gamma_{i_{1D}i_{1D}}}\frac{\gamma_{g_D i_{1D}}}{(\gamma^2_{g_D i_{1D}}+\Delta^2_{DL})(\gamma^2_{g_D i_{1D}}+\Delta^2_{DR})}, \tag{27}$$

where $\gamma_{g_D i_{1D}}=(\gamma^{(0)}_{i_{1D}i_{1D}}+\gamma_{DA})/2+\bar{\gamma}^{(0)}_{g_D i_{1D}}$. From now on, we assume that $\gamma_{g_\alpha g_\alpha}=0$, $C(\omega_{\alpha R})=\omega^4_{\alpha R}/(\pi c^4\hbar^2\varepsilon^{3/2}_\alpha)$, $\Delta_{DL}=\omega_{i_{1D}}-\omega_L$, and $\Delta_{DR}=\omega_{i_{1D}}-\omega_R$ are the detunings of the frequency of the exciting and emitting light from the frequency of the electronic transition in the donor. When the transition to state $|i_{2A}\rangle$ is optically forbidden, the acceptor luminescence cross section is given by

$$\frac{d^2\sigma^{(f)}_A}{d\Theta d\omega_{AR}} = C(\omega_{AR})|V^{(R)}_{g_A i_{1A}}|^2|V^{(L)}_{i_{1D}g_D}|^2\frac{\zeta_{i_{1A}i_{2A}}\gamma_{DA}}{\gamma_{i_{1D}i_{1D}}\gamma^{(0)}_{i_{1A}i_{1A}}\gamma^{(0)}_{i_{2A}i_{2A}}} \times \frac{\gamma_{g_D i_{1D}}}{\gamma^2_{g_D i_{1D}}+\Delta^2_{DL}}\frac{\gamma^{(0)}_{g_A i_{1A}}}{\gamma^{(0)2}_{g_A i_{1A}}+\Delta^2_{AR}}, \tag{28}$$

where $\Delta_{AR}=\omega_{i_{1A}}-\omega_R$ is the detuning of the frequency of emitted light from the frequency of the electronic transition in the acceptor, $\gamma^{(0)}_{g_D i_{1A}}=\gamma^{(0)}_{i_{1A}i_{1A}}/2+\bar{\gamma}^{(0)}_{g_A i_{1A}}$. If state $|i_{2A}\rangle$ is optically allowed, then the luminescence cross section of the acceptor can be expressed as follows:

$$\frac{d^2\sigma^{(a)}_A}{d\Theta d\omega_{AR}} = C(\omega_{AR})|V^{(R)}_{g_A i_{1A}}|^2\frac{\zeta_{i_{1A}i_{2A}}}{\gamma^{(0)}_{i_{1A}i_{1A}}\gamma^{(0)}_{i_{2A}i_{2A}}}\frac{\gamma^{(0)}_{g_A i_{1A}}}{\gamma^{(0)2}_{g_A i_{1A}}+\Delta^2_{AR}} \times \left[|V^{(L)}_{i_{2A}g_A}|^2\frac{\gamma^{(0)}_{g_A i_{2A}}}{\gamma^{(0)2}_{g_A i_{2A}}+\Delta^2_{AL}} + |V^{(L)}_{i_{D}g_D}|^2\frac{\gamma_{DA}}{\gamma_{i_{1D}i_{1D}}}\frac{\gamma_{g_D i_{1D}}}{\gamma^2_{g_D i_{1D}}+\Delta^2_{DL}}\right], \tag{29}$$

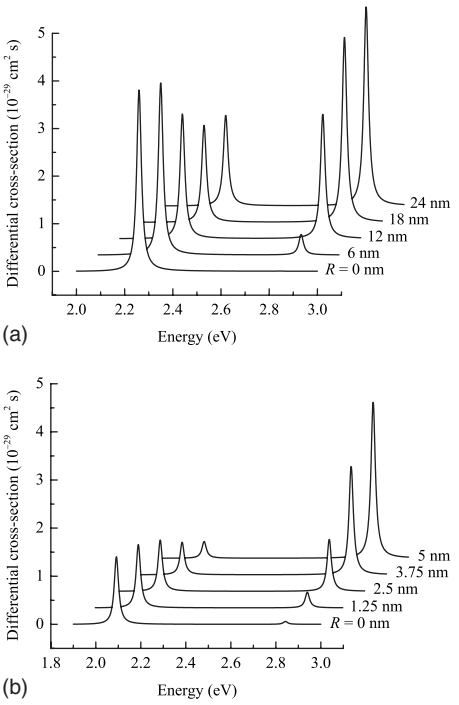

FIG. 8. Dependencies of the luminescence differential cross-section spectra of donor (right peaks) and acceptor (left peaks) on distance $R=r-(R_D+R_A)$ between the surfaces of quantum dots. (a) Dipole allowed transition in donor and acceptor. Donor: $i=i'=\{1,0,0\}$, $R_D=2$ nm. Acceptor: $f=f'=\{1,1,0\}$, $R_A=2.9$ nm. (b) Dipole allowed transition in donor and dipole-forbidden transition in acceptor. Donor: $i=i'=\{1,0,0\}$, $R_D=2$ nm. Acceptor: $f=\{1,1,0\}$, $f'=\{1,2,0\}$, $R_A=3.6$ nm.

where $\Delta_{AL}=\omega_{i_{2A}}-\omega_L$ is the detuning of the frequency of the exciting light from frequency of the electronic transition in the acceptor, $\gamma^{(0)}_{g_A i_{2A}}=\gamma^{(0)}_{i_{2A}i_{2A}}/2+\bar{\gamma}^{(0)}_{g_A i_{2A}}$.

Thus, to perform calculations using this approach, one must define seven relaxation parameters: two for the donor ($\zeta_{g_D i_{1D}}$, $\bar{\gamma}^{(0)}_{g_D i_{1D}}$) and five for the acceptor ($\zeta_{g_A i_{1A}}$, $\zeta_{g_A i_{2A}}$, $\zeta_{i_{1A}i_{2A}}$, $\bar{\gamma}^{(0)}_{g_A i_{1A}}$, $\bar{\gamma}^{(0)}_{g_A i_{2A}}$). The rate of energy transfer γ_{DA} is calculated using the results from Sec. III.

Figure 8 shows the dependence of the luminescence differential cross-section spectra on the distance between the surfaces of quantum dots when energy transfer to the energy levels of the acceptor occurs, corresponding to dipole-allowed and dipole-forbidden optical transitions. Figure 9 shows the same dependencies for the maxima of the donor and acceptor LDCS peaks. In our calculations, we used the following values for the relaxation parameters: $\zeta_{g_\alpha i_{1\alpha}}=10^8$ s^{-1}, $\zeta_{g_A i_{2A}}=10^8$ s^{-1}, $\zeta_{i_{1A}i_{2A}}=2\times10^{12}$ s^{-1}, and $\bar{\gamma}_{g_\alpha i_{1\alpha}}=\bar{\gamma}_{g_A i_{2A}}=\bar{\gamma}_{i_{1A}i_{2A}}=2\times10^{13}$ s^{-1}. For calculation of the luminescence cross-section spectrum, we used the experimentally obtained size dependence of the energy spectrum obtained in Ref. 52, allowing us to obtain spectral positions of the luminescence peaks in agreement with experiments.

For dipole-allowed transitions, the light excites both the donor and the acceptor and both the donor and acceptor peaks are visible even when the interdot distance is very large and Coulomb interaction is negligibly small. The

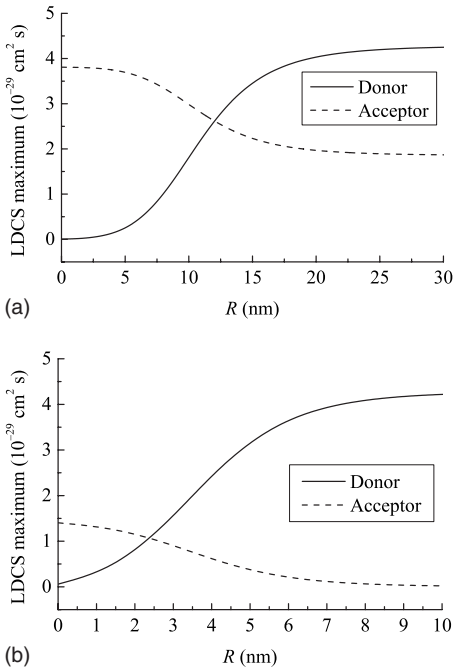

FIG. 9. Dependencies of the maxima of the donor and acceptor LDCS peaks shown in Fig. 8 on distance $R=r-(R_D+R_A)$ between the surfaces of quantum dots. (a) Dipole allowed transition in donor and acceptor. (b) Dipole-forbidden transition in acceptor.

heights of the donor and acceptor luminescence peaks differ from each other as a result of the factor $\omega_{\alpha R}^4$ present in Eqs. (27)–(29). As the distance decreases, the donor luminescence intensity reduces, while the acceptor one increases due to energy transfer. At distance comparable to the quantum dot size ($R \leqslant 5$ nm), the donor luminescence is practically quenched and the acceptor luminescence reaches its maximum intensity. In the case of dipole-forbidden transitions in the acceptor, the acceptor luminescence is absent at large interdot distance. When the distance is reduced, quenching of the donor luminescence is apparent while acceptor luminescence appears. The dissimilar distance dependencies for dipole-allowed and dipole-forbidden acceptor transitions originate in the complex distance dependence of the matrix element of Coulomb interaction. For the dipole-dipole interaction an r^{-6} law is obeyed regardless of interdot distance while the multipole interaction makes contributions proportional to higher orders of r.

V. CONCLUSION

In this work, we theoretically investigate the resonant transfer of electronic excitation energy in a system of two quantum dots. Using a two-band model and under the assumption that interaction between electrons of the quantum dot donor and quantum dot acceptor is described by a screened Coulomb potential, we obtain a relatively simple expression for the energy-transfer probability. This approach allows us to adequately consider the specific cases of short interdot distances and dipole-forbidden transitions in the acceptor. We show that the dipole-dipole approximation is valid for dipole-allowed interband transitions in the donor and acceptor even at short interdot distances. We found that the energy transfer from donor to the dipole-forbidden state of the acceptor plays an essential role in the process, and its probability can reach as high as 25% as compared to the dipole-allowed states of the acceptor.

We perform an analysis of the anisotropy of the energy transfer and show that the transfer rate strongly depends on the orientation of the dipole moments of the interband transitions and that of the radius vector connecting the quantum dot centers. Control of the orientations allows one to change the energy-transfer rate from zero to its highest possible value, suggesting that engineering of complex networks for energy transfer in ensembles of close-packed quantum dots should be possible.

We investigated the temperature dependence of the energy-transfer rate treating the energy-transfer process as an incoherent one. At the same time it has been found that the energy-transfer rate can be higher than the intraband relaxation rate in quantum dots at low temperatures. This means that for an accurate calculation of the luminescence spectrum, reverse energy transfer from the acceptor to the donor should be considered. In this case coherent effects become important resulting in the removing degeneration of resonant electronic states of donor and acceptor due to the Coulomb interaction.[8] This splitting of the energy states can cause the anticrossing in optical spectra of coupled quantum dot, for example, in external electric field that has been discussed in Ref. 8. The detailed analysis of the coherent effects and the reverse energy transfer in the quantum system at low temperature is a subject of future work. Finally, by utilizing a simple kinetic model, we obtain analytical expressions for the room-temperature luminescence spectra of quantum dot donors and acceptors with energy transfer and we also analyzed the interdot distance dependencies of these spectra.

ACKNOWLEDGMENTS

Three of the authors (S.Y.K., A.V.F., and A.V.B.) are grateful to the RFBR (Grant No. 06-02-17036a) and Ministry of Education and Science of the Russian Federation (Grant No. PHΠ2.1.1.1075) for partial financial support of this work.

APPENDIX: REPRESENTATION OF $I^{(l)}$ THROUGH APPEL HYPERGEOMETRIC FUNCTION

Interchange of the integrations in Eq. (14) allows the functions $I^{(l)}$ to be represented in the following way:

$$I^{(l)} = \left(\frac{1}{3}\right)^{l-1} \frac{2}{\pi} \sum_{l_1,l_2} \mathfrak{C}_D(l_1)\mathfrak{C}_A^*(l_2) \int_0^{R_D} \int_0^{R_A} dr_D dr_A \mathfrak{R}_D \mathfrak{R}_A Q_{l_1,l_2}^{(l)}, \tag{A1}$$

where

$$\mathfrak{C}_\alpha(l_x) = i^{l_x}(2l_x+1)\sqrt{\frac{2l_\alpha+1}{2l'_\alpha+1}} C_{l_\alpha 0, l_x 0}^{l'_\alpha 0} C_{l_\alpha m_\alpha, l_x 0}^{l'_\alpha m'_\alpha}, \tag{A2}$$

$$\Re_\alpha = \frac{2r_\alpha^2}{R_\alpha^3}\frac{j_{l_\alpha}(k_{n_\alpha l_\alpha} r_\alpha) j_{l'_\alpha}(k_{n'_\alpha l'_\alpha} r_\alpha)}{j_{l_\alpha+1}(\xi_{n_\alpha l_\alpha}) j_{l'_\alpha+1}(\xi_{n'_\alpha l'_\alpha})},$$

$$Q^{(l)}_{l_1,l_2} = \int_0^\infty dx x^l j_{l_1}(x r_D/r) j_{l_2}(x r_A/r) j_l(x), \quad l = 1,2. \quad \text{(A3)}$$

In turn $Q^{(l)}_{l_1,l_2}$ can be expressed through Appel's fourth hypergeometric function $F_4(a,b;c,c';x;y)$ (Ref. 53) in the form

$$Q^{(l)}_{l_1,l_2} = 2^{l-3}\pi^{3/2}\left(\frac{r_D}{r}\right)^{l_1}\left(\frac{r_A}{r}\right)^{l_2} \times \Gamma\begin{bmatrix} (2l+l_1+l_2+1)/2 \\ l_1+3/2, l_2+3/2, 1-(l_1+l_2)/2 \end{bmatrix} \times F_4\left(\frac{l_1+l_2}{2}, \frac{2l+l_1+l_2+1}{2}; l_1+\frac{3}{2}, l_2+\frac{3}{2}; \frac{r_D^2}{r^2}; \frac{r_A^2}{r^2}\right), \quad \text{(A4)}$$

$$\Gamma\begin{bmatrix} a \\ b,c,d \end{bmatrix} = \frac{\Gamma(a)}{\Gamma(b)\Gamma(c)\Gamma(d)}. \quad \text{(A5)}$$

From Eqs. (A4) and (A5) it follows that $I^{(l)}$ are nonzero in the following cases:

$$l_1 = l_2 = 0, \quad (l_1+l_2)/2 = \text{half-integer number}.$$

Otherwise, the argument of function $\Gamma[1-(l_1+l_2)/2]$ is zero or a negative integer and we obtain infinity. From the properties of the Clebsch-Gordan coefficients,[32] it follows that condition $l_1=l_2=0$ is satisfied only for transitions between states with the same angular momenta $l_D=l'_D$ and $l_A=l'_A$. When $l_1=l_2=0$ functions $Q^{(l)}_{l_1,l_2}$ is independent of r_D and r_A and the integrals in Eq. (A1) over these variables from $\Re_D$ and $\Re_A$ give δ_{n_D,n'_D} and δ_{n_A,n'_A}, respectively. Hence, the condition $l_1=l_2=0$ corresponds to dipole-allowed interband transitions in the donor and acceptor ($n_D=n'_D$, $l_D=l'_D$, $m_D=m'_D$, $n_A=n'_A$, $l_A=l'_A$, and $m_A=m'_A$) because according to Eq. (A2), conditions $m_D=m'_D$ and $m_A=m'_A$ must be satisfied. Moreover, in this case we have $I^{(1)}=I^{(2)}=1$.

Let us reflect on the restrictions applied by condition $(l_1+l_2)/2$=half-integer number on interband transitions in quantum dots. It is clear that this condition will be satisfied only when l_1 and l_2 have an opposite parities, i.e., when l_1=even number, l_2=odd number or l_1=odd number, l_2=even number. Since Eq. (A2) should also be satisfied, we obtain that $l_D+l'_D+l_1$=even number and $l_A+l'_A+l_2$=even number. Thus, energy transfer is only possible in two cases: (1) when interband transitions in the donor involve states with angular momenta of the same parities $l_D+l'_D$=even number and transitions in the acceptor involve states with angular momenta of opposite parities $l_A+l'_A$=odd number and (2) inversely, when $l_D+l'_D$=odd number and $l_A+l'_A$=even number. Further restrictions on the possible values of the quantum numbers of donor and acceptor states are determined by the following conditions:

$$|l_D - l_1| \le l'_D \le l_D + l_1, \quad |l_A - l_2| \le l'_A \le l_A + l_2,$$

$$m_D = m'_D, m_A = m'_A.$$

*stanislav.kruchinin@gmail.com
†a_v_fedorov@inbox.ru

[1] V. M. Agranovich and M. D. Galanin, *Spectroscopy and Excitation Dynamics of Condensed Molecular Systems* (North-Holland, Amsterdam, 1982).
[2] S. K. Lyo, Phys. Rev. B **62**, 13641 (2000).
[3] Š. Kos, M. Achermann, V. I. Klimov, and D. L. Smith, Phys. Rev. B **71**, 205309 (2005).
[4] C. R. Kagan, C. B. Murray, and M. G. Bawendi, Phys. Rev. B **54**, 8633 (1996).
[5] H. D. Robinson, B. B. Goldberg, and J. L. Merz, Phys. Rev. B **64**, 075308 (2001).
[6] S. A. Crooker, J. A. Hollingsworth, S. Tretiak, and V. I. Klimov, Phys. Rev. Lett. **89**, 186802 (2002).
[7] F. V. de Sales, S. W. da Silva, J. M. R. Cruz, A. F. G. Monte, M. A. G. Soler, P. C. Morais, M. J. da Silva, and A. A. Quivy, Phys. Rev. B **70**, 235318 (2004).
[8] A. Nazir, B. W. Lovett, S. D. Barrett, J. H. Reina, and G. A. D. Briggs, Phys. Rev. B **71**, 045334 (2005).
[9] G. D. Scholes and D. L. Andrews, Phys. Rev. B **72**, 125331 (2005).
[10] T. Pons, I. L. Medintz, M. Sykora, and H. Mattoussi, Phys. Rev. B **73**, 245302 (2006).
[11] G. Allan and C. Delerue, Phys. Rev. B **75**, 195311 (2007).
[12] D. M. Willard and A. van Orden, Nat. Mater. **2**, 575 (2003).
[13] X. Michalet, F. F. Pinaud, L. A. Bentolila, J. M. Tsay, S. Doose, J. J. Li, G. Sundaresan, A. M. Wu, S. S. Gambhir, and S. Weis, Science **307**, 538 (2005).
[14] S. Noda, Science **314**, 260 (2006).
[15] A. Imre, G. Csaba, L. Ji, A. Orlov, G. H. Bernstein, and W. Porod, Science **311**, 205 (2006).
[16] B. W. Lovett, J. H. Reina, A. Nazir, and G. A. D. Briggs, Phys. Rev. B **68**, 205319 (2003).
[17] S. Sangu, K. Kobayashi, A. Shojiguchi, and M. Ohtsu, Phys. Rev. B **69**, 115334 (2004).
[18] J. M. Taylor, H. A. Engel, W. Dür, A. Yacoby, C. M. Marcus, P. Zoller, and M. D. Lukin, Nat. Phys. **1**, 177 (2005).
[19] *Semiconductor Quantum Dots*, edited by Y. Masumoto and T. Takagahara (Springer, Germany, 2002).
[20] Th. Förster, Ann. Phys. **437**, 55 (1948).
[21] L. D. Landau and E. M. Lifshitz, *Quantum Mechanics: Non-Relativistic Theory*, Course of Theoretical Physics Vol. 3, 3rd ed. (Pergamon, Oxford, NY, 1989).
[22] D. L. Dexter, J. Chem. Phys. **21**, 836 (1953).
[23] J. Danckwerts, K. J. Ahn, J. Förstner, and A. Knorr, Phys. Rev. B **73**, 165318 (2006).
[24] T. Franzl, D. S. Koktysh, T. A. Klar, A. L. Rogach, J. Feldmann, and N. Gaponik, Appl. Phys. Lett. **84**, 2904 (2004).
[25] T. Unold, K. Mueller, C. Lienau, T. Elsaesser, and A. D. Wieck, Phys. Rev. Lett. **94**, 137404 (2005).

[26] C. de Mello Donegá, P. Liljeroth, and D. Vanmaekelbergh, Small **1**, 1152 (2005).
[27] R. Wargnier, A. V. Baranov, V. G. Maslov, V. Stsiapura, M. Artemyev, M. Pluot, A. Sukhanova, and I. Nabiev, Nano Lett. **4**, 451 (2004).
[28] A. Sukhanova, A. V. Baranov, T. S. Perova, J. H. M. Cohen, and I. Nabiev, Angew. Chem., Int. Ed. **45**, 2048 (2006).
[29] A. Franceschetti and A. Zunger, Phys. Rev. Lett. **78**, 915 (1997).
[30] E. L. Ivchenko and G. E. Pikus, *Superlattices and Other Heterostructures: Symmetry and Optical Phenomena* (Springer, Berlin, 1997).
[31] A. I. Anselm, *Introduction to Semiconductor Theory* (Prentice-Hall, Englewood Cliffs, NJ, 1978).
[32] *Quantum Theory of Angular Momentum*, edited by D. A. Varshalovich, A. N. Moskalev, and V. K. Khersonskii (World Scientific, Singapore, 1988).
[33] A. L. Efros and M. Rosen, Phys. Rev. B **58**, 7120 (1998).
[34] D. J. Norris and M. G. Bawendi, Phys. Rev. B **53**, 16338 (1996).
[35] http://www.siliconfareast.com/sio2si3n4.htm
[36] K. Vahala, IEEE J. Quantum Electron. **24**, 523 (1988).
[37] A. Al Salman, A. Tortschanoff, M. B. Mohamed, D. Tonti, F. van Mourik, and M. Chergui, Appl. Phys. Lett. **90**, 093104 (2007).
[38] F. Gindele, K. Hild, W. Langbein, and U. Woggon, J. Lumin. **87-89**, 381 (2000).
[39] S. F. Wuister, C. de Mello Donegó, and A. Meijerinka, J. Chem. Phys. **121**, 4310 (2004).
[40] V. I. Klimov and D. W. McBranch, Phys. Rev. Lett. **80**, 4028 (1998).
[41] B. Segall, in *Proceedings of the Ninth Conference on the Physics of Semiconductors*, Moscow, 1968, edited by S. M. Ryvkin (Nauka, Leningrad, 1968), p. 425.
[42] S. Rudin, T. L. Reinecke, and B. Segall, Phys. Rev. B **42**, 11218 (1990).
[43] G. Hsu and J. L. Skinner, J. Chem. Phys. **81**, 5471 (1984).
[44] T. Kümmell, R. Weigand, G. Bacher, A. Forchel, K. Leonardi, D. Hommel, and H. Selke, Appl. Phys. Lett. **73**, 3105 (1998).
[45] J. Puls, M. Rabe, H. J. Wünsche, and F. Henneberger, Phys. Rev. B **60**, R16303 (1999).
[46] M. Furis, H. Htoon, M. A. Petruska, V. I. Klimov, T. Barrick, and S. A. Crooker, Phys. Rev. B **73**, 241313(R) (2006).
[47] *Semiconductors*, Landolt-Börnstein, New Series, Group III, Vol. 17, Pt. A, edited by O. Madelung, M. Schultz, and H. Weiss (Springer, Berlin, 1982).
[48] A. V. Fedorov, A. V. Baranov, and Y. Masumoto, Opt. Spectrosc. **93**, 56 (2002).
[49] T. S. Sosnowski, T. B. Norris, H. Jiang, J. Singh, K. Kamath, and P. Bhattacharya, Phys. Rev. B **57**, R9423 (1998).
[50] V. I. Klimov, D. W. McBranch, C. A. Leatherdale, and M. G. Bawendi, Phys. Rev. B **60**, 13740 (1999).
[51] P. C. Sercel, Phys. Rev. B **51**, 14532 (1995).
[52] W. W. Yu, L. Qu, W. Guo, and X. Peng, Chem. Mater. **15**, 2854 (2003).
[53] A. P. Prudnikov, Y. A. Brychkov, and O. I. Marichev, *Special Functions*, Integrals and Series Vol. 2 (Gordon and Breach, New York, 1990).